Spectrochimica Acta Part A: Molecular and Biomolecular Spectroscopy 113 (2013) 28–36

Contents lists available at SciVerse ScienceDirect

Spectrochimica Acta Part A: Molecular and Biomolecular Spectroscopy

journal homepage: www.elsevier.com/locate/saa

IR, Raman, SERS and computational study of 2-(benzylsulfanyl)-3,5-dinitrobenzoic acid

Asha Raj [a,d], Y. Sheena Mary [b], C. Yohannan Panicker [c,*], Hema Tresa Varghese [b], K. Raju [d]

[a] Department of Physics, Government Polytechnic College, Kollam, Kerala, India
[b] Department of Physics, Fatima Mata National College, Kollam, Kerala, India
[c] Department of Physics, TKM College of Arts and Science, Kollam, Kerala, India
[d] Department of Physics, University College, Trivandrum, Kerala, India

HIGHLIGHTS

- IR, Raman and SERS were reported.
- The wavenumbers are calculated theoretically using Gaussian 09 software.
- The wavenumbers are assigned using PED analysis.
- The geometrical parameters are in agreement with that of similar derivatives.

ARTICLE INFO

Article history:
Received 2 December 2012
Received in revised form 20 April 2013
Accepted 24 April 2013
Available online 3 May 2013

Keywords:
FT-IR

GRAPHICAL ABSTRACT

FT-IR and FT-Raman spectra of IR, Raman, SERS and computational study of 2-(benzylsulfanyl)-3,5-dinitrobenzoic acid were recorded and analyzed. SERS spectra were recorded in silver colloid, silver electrode and silver substrate. The vibrational wavenumbers were computed using HF and DFT basis sets. The data obtained from wavenumber calculations are used to assign vibrational bands obtained in infrared and Raman spectra as well as in SERS of the studied molecule. Potential energy distribution of the normal modes of vibrations was done using GAR2PED program. The geometrical parameters of the title compound are in agreement with the reported similar derivatives. The presence of phenyl ring modes in the SERS spectra suggests a tilted orientation with respect to the metal surface in all cases. In all the three SERS spectra the NO2 moiety shows an enhancement, which indicates the interaction with the metal surface. The first hyperpolarizability is high and the title compound is an attractive object for future studies of nonlinear optics.

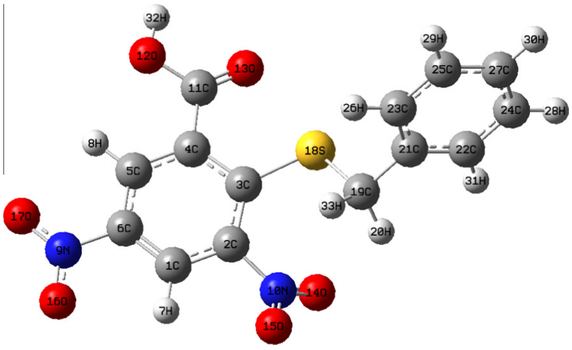

ABSTRACT

FT-IR and FT-Raman spectra of 2-(benzylsulfanyl)-3,5-dinitrobenzoic acid were recorded and analyzed. SERS spectra were recorded in silver colloid, silver electrode and silver substrate. The vibrational wavenumbers were computed using HF and DFT quantum chemical calculation methods. The data obtained from wavenumber calculations are used to assign vibrational bands obtained in infrared and Raman spectra as well as in SERS of the studied molecule. Potential energy distribution was done using GAR2PED program. The geometrical parameters of the title compound are in agreement with the reported similar derivatives. The presence of phenyl ring modes in the SERS spectra suggests a tilted orientation with

---

* Corresponding author. Tel.: +91 9895370968.
E-mail address: cyphyp@rediffmail.com (C. Yohannan Panicker).

http://dx.doi.org/10.1016/j.saa.2013.04.096

FT-Raman
SERS
DFT
Sulfanyl

respect to the metal surface in all cases. In all the three SERS spectra the NO_2 moiety shows an enhancement, which indicates the interaction with the metal surface. The first hyperpolarizability is high and the title compound is an attractive object for future studies of nonlinear optics.

Introduction

Surface Enhanced Raman Scattering (SERS) [1] is emerging as a powerful spectroscopic tool for ultra sensitive chemical analysis down to the single molecule level. The potentialities in the field of biology are enormous, for it may allow the integration of optical probes with nano/macro-structures which can then be used in applications as diverse as chemical tracing in pico-litres samples [2], micro-spectroscopy of living cells or micro-organisms and combinatorial chemistry for drug testing [3]. Sulfenyl carbonyl compounds are an interesting family of molecules related to important biological systems and the anomeric and mesomeric effects in methoxycarbonyl sulfenyl chloride is reported by Erben et al. [4]. Vallejos et al. [5] reported the experimental investigation of the structure and vibrational properties of methoxycarbonylsulfenyl isocyanate. Yang et al. [6] reported new preparation of difluoroiodomethylsulfanylbenzenes and their radical addition to unsaturated compounds initiated by sodium dithionite. Synthesis and structure activity relationships of 4-alkynyloxy phenyl sulfanyl, sulfinyl, and sulfonyl alkyl hydroxamates as tumor necrosis factor-α converting enzyme and matrix metalloproteinase inhibitors, were reported by Venkatesan et al. [7]. Pingali et al. [8] reported a highly orally bioavailable *c*-5-[6-(4-methane sulfonyloxy phenyl)-hexyl]-2-methyl-1,3-dioxane-*r*-2-carboxylic acid as a potent hypoglycemic and hypolipidemic agent. The synthesis of a series of 2-benzenesulfonylalkyl-5-substituted-sulfanyl-[1,3,4]-oxadiazoles and the examination of their anti-hepatitis B virus activity is also reported [9]. Of the different types of sulfur-centered radicals used in organic synthesis [10,11], the sulfanyl radical is one of the most attractive and its ability to add to a multiple bond intra-molecularly deserving special attraction [12] and this strategy has been successfully employed in the synthesis of alkaloids and other bioactive hetero-cycles [13–16]. Hirt et al. [17] reported the development of a practical route for the manufacture of N-[5-(3-imidazol-1-yl-4-methanesulfonyl-phenyl)-4-thiazol-2-acetamide. Aqueous chemistry of sulfenyl thiocyanates were reported by Ashby and Aneetha [18]. The role of non-bonded sulfur–oxygen interaction in the dissociative electron transfer to nitro substituted arenesulfenyl chlorides were reported by Ji et al. [19]. Important aspects of the electrochemical reduction of a series of substituted arene sulfenyl chlorides are also reported [20]. The effect of steric and electronic environments around the sulfur and nitrogen atoms and the role of non-bonded S···O/N interactions on the cyclization reactions of amide substituted benzene sulfenic acids were reported by Sarma and Mugesh [21]. Wu and Ho calculated the effect of substitutions on the region-selectivity of cyclization of α-sulfenyl-, α-sulfinyl-, and α-sulfonyl-(5R)-5-hexenyl radicals [22]. Della and Graney [23] reported the regiochemistry of cyclization of α-sulfenyl-, α-sulfinyl-, and α-sulfonyl-5-hexenyl radicals and procedures leading to region-selective syntheses of cyclic sulfones and sulfoxides. Nitro derivatives of salicylic acids as a donor in solid state coordination compounds have been studied by Lajumen et al. and the study of metal complexes with 3,5-dinitrosalicylic acid is also reported [24]. Structural confirmation of the 3,5-dinitrosalicylate anion coordination ability to metal ions have been reported by Valigura et al. [25,26] and they have reported the characterization of complex by elemental micro-analysis, electronic, IR and EPR spectra. 3,5-Dinitrosalicylic acid is an example of a proton donor having both carboxyl and hydroxyl groups, and provides one of the best chemical synthons for the construction of hydrogen-bonded structural motifs [27]. The acid has provided examples of polymorphism in which associations with solvent molecules such as water, dioxane and tert-butyl alcohol give a variety of hydrogen-bonded molecular assemblies [28,29]. SERS studies of 4-isoproppylsulfanylmethyl-1,2,3-triazole on gold surface is reported by Jbarah et al. [30]. In the present study, the IR, Raman and Surface enhanced Raman scattering spectra in silver colloid, silver electrode and in silver substrate of 2-(benzylsulfanyl)-3,5-dinitrobenzoic acid (MSDB) were investigated to get an idea regarding the orientation of the molecule on the silver surface. The vibrational wavenumbers of the title compound are also calculated theoretically and compared with experimental values. Nonlinear optics deals with the interaction of applied electromagnetic fields in various materials to generate new electromagnetic fields, altered in wavenumber, phase, or other physical properties [31]. Organic molecules able to manipulate photonic signals efficiently are of importance in technologies such as optical communication, optical computing, and dynamic image processing [32,33]. Phenyl substituents can increase molecular hyperpolarizability [34,35] a result described as surprising. Many organic molecules, containing conjugated π electrons and characterized by large values of molecular first hyperpolarizabilities, were analyzed by means of vibrational spectroscopy [36]. In this context, the hyperpolarizability of MSDB is calculated in the present study.

Experimental

Benzylsulfane (2.85 g, 23 mmol) was added to a solution of 2-chloro-3,5-dinitrobenzoic acid (5.66 g, 23 mmol) in 1,2-dimethoxyethane (DME) (25 mL) in a 100 mL flask at room temperature under argon cover gas. A solution of triethylamine (4.68 g, 46 mmol) in DME (5 mL) was then added drop wise under magnetic stirring over ca. 30 min. The mixture was stirred for 1.5 h and then poured into dilute aqueous hydrochloric acid (1:1, 20 mL). The product was extracted with chloroform (2 × 50 mL), the organic phase was dried over anhydrous sodium sulfate, and the solvent was evaporated under reduced pressure. The residue

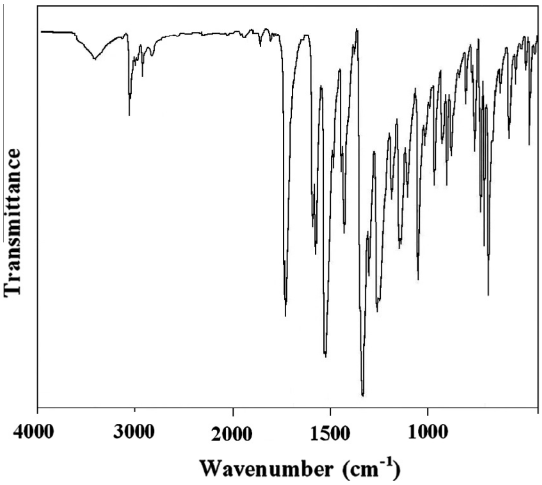

Fig. 1. FT-IR spectrum of MSDB.

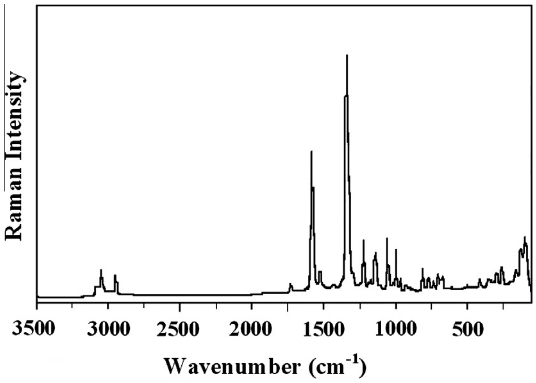

Fig. 2. FT-Raman spectrum of MSDB.

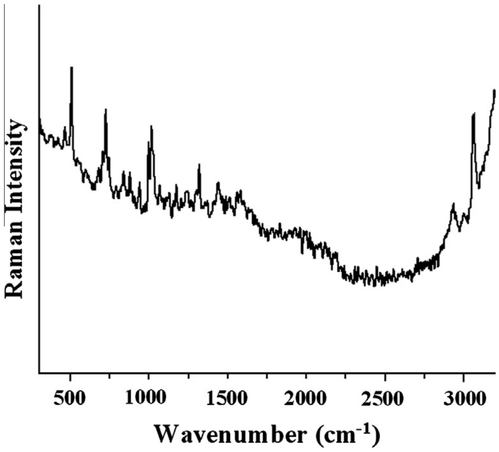

Fig. 3. SERS spectrum of MSDB in silver colloid.

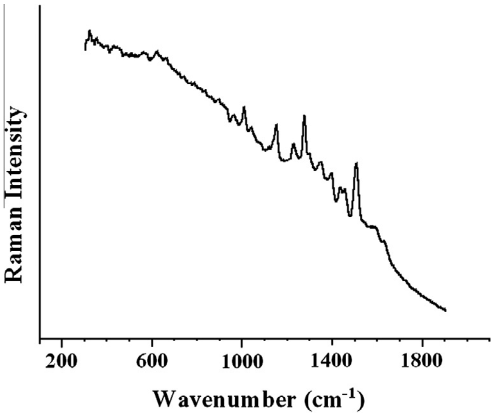

Fig. 4. SERS spectrum of MSDB in silver electrode.

was re-crystallized from methanol yielding 6.77 g (88%) of the title product.

The title compound was identified by means of ^{1}H- and ^{13}C NMR spectra, elemental analysis. The ^{1}H and ^{13}C NMR spectra were measured at 25 °C with an AMX 360 Bruker spectrometer at the frequencies of 360.14 and 90.57 MHz, respectively. For the measurements the substances were dissolved in $CDCl_3$ or $(CD_3)_2SO$ (5% solutions). The δ ^{1}H chemical shifts are referenced to the signal of HMDSO in $CDCl_3$ solutions (δ ^{1}H: 0.05) and to the solvent signal in $(CD_3)_2SO$ solutions (δ ^{1}H: 2.55). The δ ^{13}C chemical shifts are referenced to the signals of the two solvents (δ ^{13}C: 77.0 and 39.6, respectively). The analysis of the proton spectra was carried out according to the rules for the first-order splitting with the help of integral intensities. The ^{13}C NMR spectra were measured with full decoupling from the protons, and the signals were assigned with the help of SCS. The quaternary carbon atoms and CH groups were differentiated by means of the APT pulse sequence. The elemental analyses were carried out on an automatic analyzer EA 1108 (Fisons). Mp. 144–146.5 °C; yield 88%; the elemental analysis is: calculated/found (%): C 50.30/50.00, H 3.01/3.23, N 8.38/8.20, S 9.59/9.59. Chemical shifts ^{1}H (δ): H_7 8.86, H_8 8.66(d, $J = 2.5$ Hz), CH_2 4.25 s, Ph 7.40–7.14 m. ^{13}C chemical shifts (δ): C_2 154.04, C_6 146.51, C_3 140.58, C_5 134.58, C_4 129.08, C_1 120.52, CH_2 40.84, CO 166.04, C_{22} 135.89, C_{21} 135.89, C_{24} 128.78, C_{23} 128.78, C_{25} 127.95, C_{27} 126.19.

The FT-IR spectrum (Fig. 1) was recorded using a Perkin–Elmer spectrum one FT-IR spectrometer in the region 450–4000 cm^{-1} with the sample in standard KBr pellet technique. The spectral resolution was 2 cm^{-1}. FT-Raman spectra (Figs. 2 and 3) were recorded on a Bruker RFS100/s FT instrument (Nd:YAG laser, 1064 nm excitation). The aqueous silver colloid used in the SERS experiments was prepared by reduction of silver nitrate by sodium citrate, using the Lee–Meisel method [37].

Solutions of the title compound were made up in ethanol (0.1 mmol in 1 cm^3 of solvent) and transferred by a micro-syringe into the silver colloid (10 μL in 1 cm^3 of colloid) such that the overall concentration was 10^{-3} mol dm^{-3}. Colloid aggregation was induced by addition of an aqueous solution of $MgCl_2$ (1 drop of a 2 mol dm^{-3} solution). Polyvinylpyrrolidone was then used to stabilize the colloid (1 drop of 0.1 g/10 cm^3 aqueous solution). The final colloid mixture was placed in a glass tube and the Raman spectrum registered.

Electrochemical measurements were carried out with an Autolab instrument (ECO Chemie), using a conventional three electrode cell with a silver polycrystalline disk (diameter of 5 mm, 99.999% assay) as the working electrode, a large platinum sheet as the counter electrode, and a Ag/AgCl electrode in 0.1 M KCl as the reference. For Raman measurements, the silver surface for the title compound film deposition was electrochemically roughened to obtain a sufficiently enhanced intensity of the SERS bands. The silver electrode was roughened [38,39] by three successive positive–negative cycles in a 0.1 M KCl aqueous solution from −0.3 to 0.3 to −0.3 V at a sweep rate of 5 mV s^{-1}. The working silver electrode was removed at an open circuit potential and very carefully rinsed with water. Raman spectrum (Fig. 4) was recorded with an ISA T64000 Raman spectrometer equipped with three 1800 grooves/mm holographic grating and a 1024 × 256 pixel nitrogen cooled charge coupled device. The resolution of the spectrometer was ca. 1 cm^{-1}. The Raman spectrometer was also equipped with an Olympus BX 40 microscope with a 50× long distance objective

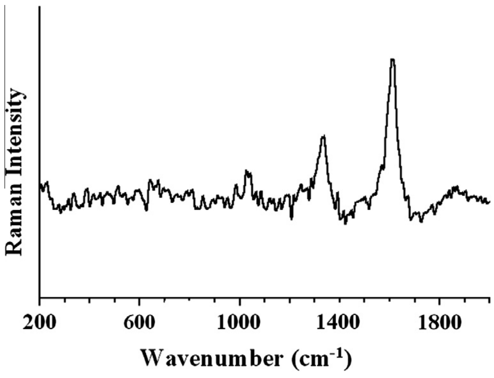

Fig. 5. SERS spectrum of MSDB in silver substrate.

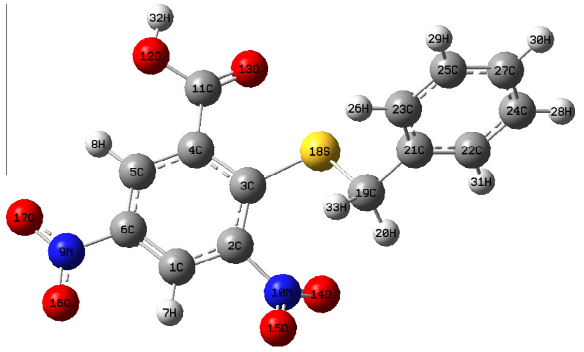

Fig. 6. Optimized geometry (B3LYP) of MSDB.

(LMPL FL 50×/0.50). A Laser Tech model LJ-800 mixed argon/krypton laser provided excitation radiations of 647.1 nm and 514.5 nm. For measurements with excitation radiation of 647.1 nm, the laser power at the sample was set below 1 mW. A band pass filter (coherent, model 35-8663 for 647.1 nm) was placed in the laser beam prior to the sample.

1.67 mgms of MSDB was dissolved in 5 mL of chloroform for recording the SERS spectrum of silver substrate (Fig. 5). Raman spectrum of MSDB as the analyte molecule was recorded on Yashnanotech's highly sensitive Raman substrate after dipping in 5 mL of 1 mM MSDB solution for 30 min [40]. The Raman spectrum was recorded on a LabRAM HR apparatus (Horiba, USA) with an excitation wavelength of 532 nm on a green laser and 5 mW cm^{-2}.

Computational details

The vibrational wavenumbers were calculated using the Gaussian 03 software package on a personal computer [41]. The computations were performed at HF/6-31G* and B3LYP/6-31G* levels of theory to get optimized geometry (Fig. 6) and vibrational wavenumbers of the normal modes of the title compound. Molecular geometry was fully optimized by Berny's optimization algorithm using redundant internal coordinates. Harmonic vibrational wavenumbers were calculated using analytic second derivatives to confirm the convergence to minima in the potential surface. At the optimized structure of the examined species, no imaginary wavenumber modes were obtained, proving that a true minimum on the potential surface was found. Scaling factors 0.8929 and 0.9613 are used for HF and DFT methods, respectively [42]. The observed disagreement between theory and experiment could be a consequence of the anharmonicity and of the general tendency of the quantum chemical methods to overestimate the force constants at the exact equilibrium geometry. The potential energy distribution (PED) is calculated with the help of GAR2PED software package [43]. The calculated geometrical parameters (DFT) are given in Table 1.

Results and discussion

The observed IR and Raman bands as well as the calculated (scaled) wavenumbers and assignments are given in Table 2.

IR and Raman spectra

The most characteristic bands in the spectra of nitro compounds are due to the NO_2 stretching vibrations, which are the two most useful group wavenumbers, not only because of their spectral positions but also for their strong intensities [44]. Nitro benzene derivatives display $\upsilon_{as}NO_2$ in the region 1535 ± 30 cm^{-1} and 3-nitro-

Table 1
Optimized geometrical (B3LYP) parameters of 2-(benzylsulfanyl)-3,5-dinitrobenzoic acid atom labeling according to Fig. 6.

Bond lengths (Å)		Bond angles (°)		Dihedral angles (°)	
C_1-C_2	1.3899	A(2,1,6)	118.7	D(6,1,2,3)	4.4
C_1-C_6	1.3857	A(2,1,7)	120.4	D(6,1,2,10)	−170.5
C_1-H_7	1.0823	A(6,1,7)	120.9	D(7,1,2,3)	−177.6
C_2-C_3	1.4179	A(1,2,3)	123.3	D(7,1,2,10)	7.6
C_2-N_{10}	1.4758	A(1,2,10)	113.7	D(2,1,6,5)	0.8
C_3-C_4	1.4318	A(3,2,10)	122.7	D(2,1,6,9)	179.4
C_3-S_{18}	1.7675	A(2,3,4)	115.4	D(7,1,6,5)	−177.3
C_4-C_5	1.3944	A(2,3,18)	125.6	D(7,1,6,9)	1.4
C_4-C_{11}	1.4906	A(4,3,18)	118.8	D(1,2,3,4)	−7.1
C_5-C_6	1.3893	A(3,4,5)	121.2	D(1,2,3,18)	168.5
C_5-H_8	1.0816	A(3,4,11)	120.8	D(10,2,3,4)	167.3
C_6-N_9	1.4667	A(5,4,11)	118.0	D(10,2,3,18)	−17.1
N_9-O_{16}	1.2302	A(4,5,6)	120.2	D(1,2,10,14)	134.4
N_9-O_{17}	1.2301	A(4,5,8)	120.2	D(1,2,10,15)	−42.2
$N_{10}-O_{14}$	1.2291	A(6,5,8)	119.6	D(3,2,10,14)	−40.5
$N_{10}-O_{15}$	1.2292	A(1,6,5)	120.9	D(3,2,10,15)	142.9
$C_{11}-O_{12}$	1.3545	A(1,6,9)	119.4	D(2,3,4,5)	5.0
$C_{11}-O_{13}$	1.2132	A(5,6,9)	119.7	D(2,3,4,11)	−173.7
$O_{12}-H_{32}$	0.9754	A(6,9,16)	117.4	D(18,3,4,5)	−170.9
$S_{18}-C_{19}$	1.8641	A(6,9,17)	117.4	D(18,3,4,11)	10.3
$C_{19}-H_{20}$	1.0903	A(16,9,17)	125.2	D(2,3,18,19)	−24.2
$C_{19}-C_{21}$	1.5072	A(2,10,14)	117.3	D(4,3,18,19)	151.3
$C_{19}-H_{33}$	1.0940	A(2,10,15)	117.4	D(3,4,5,6)	−0.4
$C_{21}-C_{22}$	1.4008	A(14,10,15)	125.2	D(3,4,5,8)	178.8
$C_{21}-C_{23}$	1.4019	A(4,11,12)	112.7	D(11,4,5,6)	178.4
$C_{22}-C_{24}$	1.3955	A(4,11,13)	124.9	D(11,4,5,8)	−2.4
$C_{22}-H_{31}$	1.0874	A(12,11,13)	122.3	D(3,4,11,12)	−165.8
$C_{23}-C_{25}$	1.3936	A(11,12,32)	106.0	D(3,4,11,13)	15.3
$C_{23}-H_{26}$	1.0875	A(3,18,19)	105.7	D(5,4,11,12)	15.5
$C_{24}-C_{27}$	1.3954	A(18,19,20)	109.3	D(5,4,11,13)	−163.4
$C_{24}-H_{28}$	1.0865	A(18,19,21)	107.3	D(4,5,6,1)	−2.7
$C_{25}-C_{27}$	1.3971	A(18,19,33)	108.4	D(4,5,6,9)	178.7
$C_{25}-H_{29}$	1.0866	A(20,19,21)	111.2	D(8,5,6,1)	178.1
$C_{27}-H_{30}$	1.0865	A(20,19,33)	109.1	D(8,5,6,9)	−0.5
		A(21,19,33)	111.4	D(1,6,9,16)	1.5
		A(19,21,22)	120.1	D(1,6,9,17)	−178.6
		A(19,21,23)	120.9	D(5,6,9,16)	−179.9
		A(22,21,23)	118.9	D(5,6,9,17)	0.0
		A(21,22,24)	120.6	D(4,11,12,32)	−177.3
		A(21,22,31)	119.5	D(13,11,12,32)	1.6
		A(24,22,31)	119.9	D(3,18,19,20)	85.8
		A(21,23,25)	120.6	D(3,18,19,21)	−153.5
		A(21,23,26)	119.5	D(3,18,19,33)	−33.0
		A(25,23,26)	119.9	D(18,19,21,22)	−94.2
		A(22,24,27)	120.1	D(18,19,21,23)	85.4
		A(22,24,28)	119.8	D(20,19,21,22)	25.4
		A(27,24,28)	120.2	D(20,19,21,23)	−155.0
		A(23,25,27)	120.1	D(33,19,21,22)	147.3
		A(23,25,29)	119.8	D(33,19,21,23)	−33.1
		A(27,25,29)	120.1	D(19,21,22,24)	−180.0
		A(24,27,25)	119.8	D(19,21,22,31)	−0.4
		A(24,27,30)	120.1	D(23,21,22,24)	0.4
		A(25,27,30)	120.1	D(23,21,22,31)	180.0
				D(19,21,23,25)	179.8
				D(19,21,23,26)	0.1
				D(22,21,23,25)	−0.6
				D(22,21,23,26)	179.6
				D(21,22,24,27)	−0.0
				D(21,22,24,28)	179.8
				D(31,22,24,27)	−179.7
				D(31,22,24,28)	0.1
				D(21,23,25,27)	0.4
				D(21,23,25,29)	−179.5
				D(26,23,25,27)	−179.8
				D(26,23,25,29)	0.3
				D(22,24,27,25)	−0.1
				D(22,24,27,30)	179.8
				D(28,24,27,25)	−179.9
				D(28,24,27,30)	−0.0
				D(23,25,27,24)	−0.1
				D(23,25,27,30)	−180.0
				D(29,25,27,24)	179.9
				D(29,25,27,30)	−0.0

Table 2
Calculated vibrational wavenumbers (scaled), measured infrared, Raman bands and assignments of 2-(benzylsulfanyl)-3,5-dinitrobenzoic acid.

$\upsilon_{(HF)}$ (cm^{-1})	$\upsilon_{(DFT)}$ (cm^{-1})	$\upsilon_{(IR)}$ (cm^{-1})	$\upsilon_{(Raman)}$ (cm^{-1})	$\upsilon_{(SERS)}$ (cm^{-1}) C	$\upsilon_{(SERS)}$ (cm^{-1}) E	$\upsilon_{(SERS)}$ (cm^{-1}) S	Assignments[a]
3615	3554	3498	–	–	–	–	υOH(100)
3089	3147	–	–	–	–	–	υCHII(99)
3083	3140	–	–	–	–	–	υCHII(99)
3028	3089	3086	–	3070	–	–	υCHI(92)
3018	3079	–	–	–	–	–	υCHI(99)
3008	3070	3069	3070	3060	–	–	υCHI(95)
3000	3061	–	3063	–	–	–	υCHI(94)
2996	3058	–	–	–	–	–	υCHI(100)
2995	3041	3035	–	–	–	–	υ$_{as}$CH$_2$(99)
2918	2969	2967	2960	2990	–	–	υ$_s$CH$_2$(99)
1818	1748	1742	1745	–	–	1702	υC=O(76)
1674	1601	1621	1604	–	1617	1610	υ$_{as}$NO$_2$(62) υPhII(30)
1657	1599	1598	–	–	–	–	υPhI(71)
1617	1585	1582	1588	1575	–	–	υ$_{as}$NO$_2$(74)
1597	1581	–	–	–	–	–	υPhI(75)
1596	1561	–	–	1554	1557	1566	υPhII(44) υ$_{as}$NO$_2$(32) δCHII(14)
1564	1532	1526	1538	–	1528	–	υPhII(56) υ$_{as}$NO$_2$(25)
1492	1486	1494	–	1502	1500	1485	υPhI(64) δCHI(22)
1485	1460	1466	–	–	–	–	δCH$_2$(86)
1474	1444	1431	1440	1432	1449	–	δCHI(45) υPhI(24)
1470	1394	–	1390	–	1394	1387	δCHII(20) υPhII(60)
1448	1379	1379	–	–	–	–	δCHII(42) υPhII(49)
1417	1347	–	–	1353	1353	–	υ$_s$NO$_2$(54) υPhII(22)
1394	1343	–	1343	–	–	–	υ$_s$NO$_2$(53) υCO(46)
1347	1332	1328	–	1319	–	1335	υ$_s$NO$_2$(76)
1328	1317	–	–	–	–	–	δCHI(84)
1274	1309	1309	1310	–	1293	–	υPhI(82)
1216	1291	1264	–	–	1272	1278	υPhII(77)
1207	1232	1224	1233	1233	1224	1240	δCH$_2$(82)
1195	1187	1190	1190	–	1183	1187	υCC(43) δPhI(12) υPhI(22)
1179	1178	–	–	–	–	–	δOH(31) υCC(14) δPhII(14)
1167	1168	–	–	1172	1171	–	υPhI(12) δCHI(77)
1164	1166	–	–	–	–	–	δCHII(52) υPhII(26)
1147	1149	1152	1150	–	1144	–	δCHI(78) υPhI(14)
1133	1129	1138	–	–	–	1124	δCH$_2$(66)
1109	1118	1113	1110	1120	1112	–	υCO(49) δOH(25)
1074	1087	–	–	–	1077	1079	δCHII(29) υPhII(29) υCO(12) υCS(10)
1058	1065	1062	1064	1066	1058	1065	δCHI(27) υPhI(38) δCH$_2$(11)
1038	1032	1025	1027	–	–	1028	δPhII(43) υPhII(13) υCS(18)
1010	1017	1000	1010	1016	1011	–	δCHI(12) υPhI(67)
1008	979	975	972	996	–	984	δPhI(68) υPhI(19)
984	962	–	–	–	962	–	γCHI(85) τPhI(14)
981	935	938	942	–	–	946	γCHII(74) τPhII(12)
974	932	931	–	–	–	–	γCHI(91)
968	922	–	–	–	–	–	γCHII(68) τPhII(11)
946	914	912	910	–	914	–	υCN(35) δNO$_2$(17) δPhII(11) γCHII(10)
934	897	890	897	–	–	–	γCHI(77) τPhI(11)
902	884	880	–	–	–	–	δCH$_2$ (52) υCN(40)
885	872	868	–	877	–	851	δCH$_2$(76)
854	826	828	824	836	843	–	γCHI(100)
813	802	793	796	–	–	806	υCC(22) δPhI(20) υPhI(17)
795	775	785	788	780	787	785	δNO$_2$(58) δPhII(23)
792	761	759	–	–	–	765	γCO(25) τPhII(17) γCC(16) γCS(10)
791	756	–	754	–	–	–	τPhI(35) γCC(24) γCHI(27)
771	750	741	750	–	753	–	γNO$_2$(54) γCN(29)
761	725	737	–	736	739	–	δNO$_2$(49) δPhII(35)
744	718	707	712	703	–	701	γNO$_2$(48) γCN(14) τPhII(16)
710	686	690	690	–	–	–	γCHI(36) τPhI(48)
700	685	680	–	676	681	–	γCN(16) τPhII(42) γCS(14)
685	667	655	655	–	–	669	τPhI(44) υCS(38)
651	634	640	–	–	–	638	δCO(37) τPHII(20) υCS(38)
628	617	621	622	–	–	–	τCOOH(22) δCO(28) δCN(23)
608	611	–	–	–	–	–	δPhI(87)
590	596	586	–	–	599	–	τCCOH(26) δCC(13) δCO(11) υCS(11)
571	571	–	–	588	–	585	τCCOH(43) τPhII(40)
553	552	552	–	–	–	536	δPhI(49) τPhII(23)
527	518	517	–	532	523	–	δCN(43)
505	500	509	505	509	–	508	τPhII(48) γCN(17) γCS(16)
482	476	483	–	462	–	466	τPhI(54) γCC(33)
454	459	448	455	–	447	449	τPhII(49) γCN(36)
418	403	–	429	416	420	414	τPhII(48) δCN(34)
406	400	–	395	360	373	386	τPhI(83)
357	357	–	350	–	357	–	τPhII(39) δPhII(39)
333	341	–	340	–	–	–	δCC19C(63)

Table 2 (*continued*)

$\upsilon_{(HF)}$ (cm^{-1})	$\upsilon_{(DFT)}$ (cm^{-1})	$\upsilon_{(IR)}$ (cm^{-1})	$\upsilon_{(Raman)}$ (cm^{-1})	$\upsilon_{(SERS)}$ (cm^{-1}) C	$\upsilon_{(SERS)}$ (cm^{-1}) E	$\upsilon_{(SERS)}$ (cm^{-1}) S	Assignments[a]
330	327	–	–	–	320	333	δPhII(66)
317	317	–	–	–	–	312	δCSC(22) δCO(16) δCN(29)
303	305	–	298	–	–	–	δPhII(51)

[a] υ – stretching; δ – in-plane deformation; γ – out-of-plane deformation; τ – torsion; PhI – mono substituted phenyl ring; PhII – poly substituted phenyl ring; % of PED is given in the brackets; C – silver colloid; E – silver electrode; S – silver substrate.

pyridines [44,45] at 1530 ± 20 cm^{-1}. In substituted nitrobenzenes [44,45] υ_sNO_2 appears strongly at 1345 ± 30 cm^{-1}. The bands seen at 1604, 1588, 1538 cm^{-1} in the Raman spectrum and 1621, 1582, 1526 cm^{-1} in the IR spectrum are assigned as $\upsilon_{as}NO_2$ for the title compound. The calculated values (DFT) for these modes are 1601, 1585, 1561, 1532 cm^{-1}. The band observed at 1343 cm^{-1} in the Raman spectrum and 1328 in the IR spectrum and 1347, 1343, 1332 cm^{-1} (calculated) are assigned as the υ_sNO_2 modes. Sundaraganesan et al. [46] reported the asymmetric and symmetric NO_2 stretching modes at 1600, 1571 cm^{-1} and at 1371, 1319 cm^{-1}, respectively.

When conjugated to C=C or aromatic molecules, the NO_2 scissors occur at higher wavenumbers (850 ± 60 cm^{-1}). In aromatic compounds the wagging mode ωNO_2 is assigned at 740 ± 50 cm^{-1} with a moderate to strong intensity [44]. The rocking mode ρNO_2 is active in the region 540 ± 70 cm^{-1} in aromatic nitro compounds [44]. The deformation modes of NO_2 are reported at 744 (IR), 703, 716 (DFT), 839 (Raman), 821 cm^{-1} (DFT) [46]. The bands at 910, 788, 750, 712 cm^{-1} in the Raman spectrum and at 912, 785, 741, 737, 707 cm^{-1} in the IR spectrum are the deformation modes of NO_2 and the calculated values are 914, 775, 750, 725, 718 cm^{-1}.

The vibrations of the CH_2 group, the asymmetric stretch $\upsilon_{as}CH_2$, symmetric stretch υ_sCH_2, scissoring vibration δCH_2 and wagging vibration ωCH_2 appear in the regions 3000 ± 50, 2965 ± 30, 1455 ± 55 and 1350 ± 85 cm^{-1} respectively [44,47]. The DFT calculations give $\upsilon_{as}CH_2$ at 3041 and υ_sCH_2 at 2969 cm^{-1}. The band observed at 1466 cm^{-1} in the IR spectrum and 1460 cm^{-1} calculated value are assigned as the scissoring modes δCH_2. The CH_2 wagging modes are observed at 1224 cm^{-1} in the IR spectrum, 1233 in Raman spectrum and at 1232 cm^{-1} theoretically. The bands 1138 cm^{-1} in IR and 1129 cm^{-1} (calculated) are assigned as the twisting mode of CH_2. The rocking mode [44] ρCH_2 is expected in the range 895 ± 85 cm^{-1}. The bands at 884 and 872 cm^{-1} (DFT) are assigned as ρCH_2 modes for the title compound. The torsion modes of CH_2 and NO_2 are seen in the low wavenumber range [44].

The C=O stretching vibration in the spectra of carboxylic acids [44] give rise to a band in the region 1725 ± 65 cm^{-1}. In the present case, we have observed a band at 1742 cm^{-1} in the IR spectrum, 1745 cm^{-1} in Raman spectrum and 1748 cm^{-1} theoretically. Two bands arising from the C—O stretching and OH bending appear in the spectra of carboxylic acids near 1320–1210 cm^{-1} and 1440–1395 cm^{-1}, respectively [48]. Both of these bands involve some interaction between C—O stretching and in-plane C—O—H bending. The $\upsilon(C—O)_c$ mode is reported at 1377 cm^{-1} for sodium salicylate [49], at 1391 cm^{-1} for 4-aminosalicylic acid [50] and at 1375 (IR), 1382 cm^{-1} (HF) for 3,5-dinitrosalicylic acid [51]. For the title compound, the band observed at 1343 cm^{-1} (DFT) and 1343 cm^{-1} (Raman) is assigned as $\upsilon(C—O)_c$ mode and this mode is not pure, but contains significant contributions from other modes.

Since the identification of all the normal modes of vibration of large molecules is not trivial, we tried to simplify the problem by considering each molecule as substituted benzene. Such an idea has already been utilized by several workers for the vibrational assignments of molecules containing multiple, homo- and hetero-aromatic rings [52–56]. In the following discussion, the mono and poly substituted phenyl rings are designated as PhI and PhII, respectively. In poly substituted benzenes, the aromatic CH stretching vibrations [44,57] absorb between 3000 and 3120 cm^{-1}. The DFT calculations give bands in the range 3058–3147 cm^{-1}.

The benzene ring possesses six ring-stretching vibrations, of which the four with the highest wavenumbers (occurring near 1600, 1580, 1490 and 1440 cm^{-1}) are good group vibrations [44] With heavy substituents, the bands tend to shift to somewhat lower wavenumbers. In the absence of ring conjugation [44], the band at 1580 cm^{-1} is usually weaker than that at 1600 cm^{-1}. In the case of C=O substitution, the band near 1490 cm^{-1} can be very weak [44]. The fifth ring stretching vibration is active near 1315 ± 65 cm^{-1}, a region that overlaps strongly with that of the CH in-plane deformation [44]. The sixth ring stretching vibration, or the ring breathing mode appears as a weak band near 1000 cm^{-1} in mono, 1,3-di- and 1,3,5-trisubstituted benzenes. In the otherwise substituted benzenes, however, this vibration is substituent sensitive and difficult to distinguish from the ring in-plane deformation [44]. The DFT calculations give υPh modes in the range 1309–1599 for PhI and 1291–1601 cm^{-1} for PhII, as expected [44].

The aromatic CH out-of-plane deformations [44] are observed in the range 720–1000 cm^{-1}. The spectral positions of the weaker γCH near 900 cm^{-1} correlates well with electron donating or electron attracting properties of the substituent. The CH in-plane deformations δCH are obtained at 1431, 1379, 1152, 1062, 1000 cm^{-1} in the IR spectrum and at 1440, 1390, 1150, 1064, 1010 cm^{-1} in the Raman spectrum. The DFT calculation gave in-plane CH modes of the phenyl rings in the range 1017–1444 cm^{-1}. The out-of-plane deformations and in-plane deformation of the phenyl ring [44] are observed below 1000 cm^{-1} and these modes are not pure but contain a significant contribution from other modes and are substituent sensitive. The ring breathing mode appears as a weak band near 1000 cm^{-1}, in mono-, 1,3-di- and 1,3,5-tri substituted benzenes [44]. In the otherwise substituted benzenes however, this vibration is substituent sensitive and difficult to distinguish from the ring in-plane deformation [44]. For the title compound the ring breathing mode appears at 1000 cm^{-1} in the IR spectrum, 1010 cm^{-1} in the Raman spectrum, and at 1017 cm^{-1} theoretically for PhI and at 1025 cm^{-1} in IR, 1027 cm^{-1} in Raman spectrum, 1032 cm^{-1} theoretically for PhII. Aromatic nitro compounds show a C—N stretching vibration [48,58] near 870 cm^{-1}. In the present study, the υCN is 910 cm^{-1} in the Raman spectrum and at 914, 884 cm^{-1} theoretically.

Geometrical parameters and first hyperpolarizability

To the best of our knowledge, no X-ray crystallographic data of MSDB has yet been established. However, the theoretical results obtained are almost comparable with the reported structural parameters of similar molecules. In the present case, the carbon-sulfur bond lengths $C_3—S_{18}$ = 1.7675 and $C_{19}—S_{18}$ = 1.8641 Å, while the reported values are 1.7846 (XRD), 1.792 (MP2), 1.811 Å (DFT) and 1.771 (XRD), 1.803 (DFT), 1.783 Å (MP2) [5]. The aromatics rings of the title compound are some what irregular and the spread of the CC bond distance is 1.3936–1.4019 Å for ring I and 1.3857–1.4318 Å for ring II, which is similar to the spread reported by Smith et al. [28].

For the title compound, the C—N bond lengths are 1.4758, 1.4667 Å and N—O bond lengths are in the range 1.2302–1.2291 Å, which are in agreement with the reported values. Chambers et al. [59] reported the N—O bond lengths in the range

1.2201–1.2441 Å and C—N length as 1.4544 Å. The experimental values of N—O bond lengths are 1.222–1.226 Å and C—N lengths in the range 1.442–1.460 Å [60]. Sundaraganesan et al. [46] reported C—N bond lengths as 1.453, 1.460 Å (DFT) and N—O bond lengths in the range 1.228–1.248 Å. The CNO angles are reported [46] in the range 117.4–118.7° where as for the title compound, the range is 117.4–117.3°. The DFT calculations give shortening of angle C_4—C_3—S_{18} by 1.2° and increase of angle C_2—C_3—S_{18} by 5.6° from 120° at C_3 position and this asymmetry of exocyclic angles reveal the repulsion between carboxylic group and the phenyl ring II [61]. DFT calculations give the shortening of the angle C_1—C_2—N_{10} by 6.3° and the increase of angle C_3—C_2—N_{10} by 2.7° from 120° at C_2 position and this asymmetry of exocyclic angle, reveal the hydrogen bonding with H_7, which is evident from the enlargement in the angle C_1—C_2—C_3 by 3.3°. At C_6 position the exocyclic angles are nearly the same (119.4, 119.7°).

For the carboxylic group, the bond angles O_{12}—C_{11}—O_{13} = 122.3, O_{12}—C_{11}—C_4 = 112.7, O_{13}—C_{11}—C_4 = 124.9, C_{11}—O_{12}—H_{32} = 106.0° which are similar to the reported values [62]. For the title compound C_{11}—O_{13} = 1.2132, C_{11}—O_{12} = 1.3545, O_{12}—H_{32} = 0.9754 Å and the corresponding reported values are 1.203, 1.361, 0.965 Å [63]. The carbon–oxygen distance unambiguously define the single and double bonds in the carboxylate group and are in agreement with the values given by Ng et al. [64] For the carboxyl group, Kaduk [65] reported C_4—C_{11} = 1.481 and the in the present case the corresponding value is 1.4906 Å.

The sulfanyl moiety is twisted from the phenyl ring II and Phenyl ring I as is evident from the torsional angles, C_5—C_4—C_3—S_{18} = −170.9, C_4—C_3—S_{18}—C_{19} = 151.3, C_2—C_3—S_{18}—C_{19} = −24.2, C_1—C_2—C_3—S_{18} = 168.5 and C_{23}—C_{21}—C_{19}—S_{18} = 85.4, C_{25}—C_{23}—C_{21}—C_{19} = 179.8, C_{24}—C_{22}—C_{21}—C_{19} = −180.0, C_{22}—C_{21}—C_{19}—S_{18} = −94.2°. At C_4 position, C_3—C_4—C_{11} is increased by 0.8° and C_5—C_4—C_{11} is reduced by 2° from 120° which show the interaction between O_{13} and S_{18} atoms.

Analysis of organic molecules having conjugated π-electron systems and large hyperpolarizability using infrared and Raman spectroscopy has been evolved as a subject of research [66]. The first hyperpolarizability (β_0) of this novel molecular system is calculated theoretically, based on the finite field approach. In the presence of an applied electric field, the energy of a system is a function of the electric field. First hyperpolarizability is a third rank tensor that can be described by a 3 × 3 × 3 matrix. The 27 components of the 3D matrix can be reduced to 10 components due to the Kleinman symmetry [67].

The components of β are defined as the coefficients in the Taylor series expansion of the energy in the external electric field. When the electric field is weak and homogeneous, this expansion becomes

$$E = E_0 - \sum_i \mu_i F^i - \frac{1}{2}\sum_{ij} \alpha_{ij} F^i F^j - \frac{1}{6}\sum_{ijk} \beta_{ijk} F^i F^j F^k - \frac{1}{24}\sum_{ijkl} \gamma_{ijkl} F^i F^j F^k F^l + \ldots$$

where E_0 is the energy of the unperturbed molecule, F^i is the field at the origin, μ_i, α_{ij}, β_{ijk} and γ_{ijkl} are the components of dipole moment, polarizability, the first hyper polarizabilities, and second hyperpolarizibilities, respectively. The calculated first hyperpolarizability of the title compound is 8.86×10^{-30} esu, which is comparable with the reported values of similar derivatives [68] and experimental evaluation of this data is not readily available. We conclude that the title compound is an attractive object for future studies of nonlinear optical properties.

RMS values of wavenumbers were evaluated using the following expression [69].

$$\mathrm{RMS} = \sqrt{\frac{1}{n-1}\sum_i^n \left(\upsilon_i^{\mathrm{calc}} - \upsilon_i^{\mathrm{exp}}\right)^2}$$

The RMS error of the observed Raman bands is 33.31, 10.13 and that for IR bands is 33.57, 11.08, respectively, for HF and DFT calculations.

SERS in silver colloid

In the SERS spectrum of the title compound, the aromatic C—H stretching vibrations are observed at 3070 and 3060 cm^{-1} as weak bands for the phenyl ring PhI, which suggests that the ring PhI may be in a position close to the perpendicular to the silver surface [70–72], possibly a tilted position since it is a weak band. It has also been documented in the literature [73] that when a benzene ring moiety interacts directly with a metal surface, the ring breathing mode has to be red-shifted by ∼10 cm^{-1} along with substantial band broadening in the SERS spectrum. Neither a substantial red shift nor significant band broadening was identified in the SERS spectrum of the title compound implying that the probability of a direct ring π-orbital to metal interaction should be low, in accordance with a tilted position of the ring PhI.

In the SERS spectrum of 2-amino,5-nitropyrimidine [74], the symmetric NO_2 stretching mode corresponds to the most intense band, which appears broad and significantly downshifted from 1344 to 1326 cm^{-1}, suggesting a binding to the silver through the lone pairs of the oxygen atom. Carrasco et al. [75] observed the $\upsilon_{as}NO_2$ band in the SERS spectrum at ∼1500 cm^{-1} with medium intensity, which demonstrates the importance of nitro group in regard to the interaction with the metal. Further, they observed the enhancement of υPh modes revealing that the molecule is oriented perpendicular to the metal surface, whereas the changes that occur in the nitro group indicate that the interaction occurs through O atoms of the nitro moiety. The interaction induces a π electronic redistribution primarily around both the nitro group and the aromatic portion in the vicinity of the substitution site. Gao and Weaver [76] observed broadening and downshift of the corresponding band of nitrobenzene adsorbed on gold via the nitro group. In the SERS spectrum of p-nitroaniline, the υPh vibration at 1597 cm^{-1} is very strong, indicating the interaction between benzene ring and the metal surface. Also, a strong enhancement is observed [77] for the symmetric stretching mode of NO_2 at 1336 cm and the wagging mode of NO_2 at 865 cm^{-1}.

For the title compound the symmetric stretching mode of NO_2 is seen at 1319 cm^{-1} in the SERS spectrum which is absent in the normal Raman spectrum, whereas the computed value is 1332 cm^{-1}. A charge transfer from the oxygen atoms of the NO_2 group to the metal is evidenced by the marked downshift of the symmetric stretching of the NO_2 group as is detected by the SERS spectrum [74–77]. Interaction through the NO_2 group was also supported by the presence of modes at 1575, 1554, 1353, 780, 736, 703, 532, 509 cm^{-1} in the SERS spectrum. According to surface selection rule, vibrations involving atoms that are close to the silver surface will be enhanced [78,79]. The in-plane bending modes δCH of the aromatic ring PhI are observed at 1432, 1172, 1066 cm^{-1} in the SERS spectrum. The presence of these modes suggests that the benzene ring PhI is oriented tilted to the silver surface [78,79]. Also υPhI modes observed at 1502, 1432, 1172, 1066 cm^{-1} in the SERS spectrum supports this fact. According to the surface selection rules [80,81], the presence of in-plane vibrational modes at 1172, 1066, 996 cm^{-1} and of the out-of-plane vibrational modes at 836, 462 cm^{-1} in the SERS spectrum of the title compound suggest that there is a certain angle between the ring PhI and the surface of the silver particle. The substituent sensitive in-plane and out-of-plane modes are also detected at the same time for the ring PhI, suggesting a tilted orientation of the molecule [49,82]. In the case of SERS spectrum of thymine molecules on silver [83], the deformation band of the methyl group attached with the phenyl ring is present at 1355 cm^{-1} with the position of the methyl group close to the metallic surface. In 2-methyl pyridine, Bunding et al. [84] noticed significant shift and broadening of the CH_3 modes in the SERS spectrum. They explained this in terms of the interaction of the methyl group with the metal surface. In the present study, the CH stretching of the CH_2 group attached with the phenyl ring PhI is observed at 2990 cm^{-1}. It should be related to the closeness of the CH_2 group to the silver surface. This is justifiable because the modes in groups directly interacting with the metal surface will be prominent in the SERS spectrum and undergo a wavenumber shift [85]. Further, the CH_2 bands at 1233, 1066, 877 cm^{-1} are also observed in the SERS spectrum thereby supporting the above argument.

SERS spectrum in silver electrode

The SERS spectrum of the title compound (0.1 M) on silver electrode in 0.1 M KCl was recorded in the wavenumber range 600–2000 cm^{-1} at an electrode potential 0.1 V.

In this case, the symmetric stretching of NO_2 is seen at 1353 cm^{-1} in the SERS spectrum, which is absent in the normal Raman spectrum and upshifted from the computational value 1347 cm^{-1}, which indicates that the nitro group is not subjected to change upon the surface adsorption of the title compound on silver, as reported by Han et al. [86]. Interaction through the nitro group was also supported by the presence of bands at 1617, 1557, 1528, 914, 787, 753, 739, 681, 523, 447, 420 cm^{-1} in the SERS spectrum.

The in-plane bending modes δCH 1449, 1171, 1144, 1058, 1011 cm^{-1} and 1394, 1077 cm^{-1} are present in SERS spectrum for the aromatic rings PhI and PhII, respectively. Also the out-of-plane ring CH bending modes γCH are present in the SERS spectrum at 962, 843 cm^{-1} and at 914 cm^{-1} for ring PhI and PhII, respectively. The bending modes of phenyl ring are observed at 962 cm^{-1} for PhI and at 914, 787, 739, 681, 447, 420, 357, 320 cm^{-1} for PhII indicates change in orientation in this case. Also, the benzene ring vibrations present at 1500, 1293, 1183, 1171, 1058, 1011 cm^{-1} for PhI and at 1557, 1528, 1394, 1353, 1272, 1077 cm^{-1} for PhII in the SERS spectrum on silver electrode support this argument. In the potential dependent SERS spectrum of pyrazine adsorbed on silver substrate, the ring stretching modes are upshifted and this indicates that the adsorption of pyrazine on the substrate is quite strong [87]. Neto et al. [88] reported marked upshifts and small downshifts with respect to the corresponding Raman bands on the free molecule, and for salicylic acid there is an upshift for the ring stretching modes in the SERS spectrum [89]. Sajan et al. [90] reported phenyl ring stretching mode at 1618 and 1585 cm^{-1} in the SERS spectrum and at 1604 and 1577 cm^{-1} in the normal Raman spectrum for methyl-3-(4-methoxyphenyl)prop-2-enoate and the ring modes are blue shifted with substantial band broadening in the SERS spectrum. This indicates the direct interaction between the benzene ring moiety with metal surface, as well documented in literature [91–93] and the probability of direct ring π-orbital to metal interaction should be high [94–96]. This can be interpreted as the bond weakening in the benzene ring system caused by the back donation of the metal d electrons to the benzene ring antibonding π^* orbitals [96]. Liu [97] also reported the upshift of stretching modes on roughened metal surfaces. In the present case also, the ring stretching modes in the SERS spectrum shows such variations.

SERS spectrum on substrate

In this case also, the NO_2 bands are present at 1610, 1566, 1335, 785, 701 cm^{-1} which shows the interaction between NO_2 moiety and the metal surface. The in-plane bending modes δCH of the aromatic ring are observed at 1065 cm^{-1} for PhI and at 1387, 1079 cm^{-1} for PhII rings. The presence of these modes suggests that the benzene rings are tilted with respect to the silver surface [78,79]. The benzene ring vibrations observed at 1610, 1566, 1387, 1278, 1079, 1028 cm^{-1} for PhII and 1485, 1187, 1065 cm^{-1} for PhI rings in the SERS spectrum support this fact. Also the out-of-plane γCH vibration is present at 946 cm^{-1} for the ring PhII. The phenyl ring deformation bands are present in the SERS spectrum at 984, 806, 669, 536, 466, 386, 222 cm^{-1} for PhI and at 1028, 765, 701, 638, 585, 508, 449, 414, 333 cm^{-1} for PhII ring which show that both the phenyl rings are tilted with the metal surface. Kwon et al. [98] reported the vibrational spectroscopic investigations of benzoic acid and 4-methylbenzoic acid adsorbed on silver sol and silver electrode and proposed different orientations based on the different surface morphologies along with intrinsic difference in the nature of SERS active sites on the two surfaces. Wang et al. [99] and Podstawka et al. [100] also reported similar orientation and adsorption changes in silver colloid and silver electrode.

Conclusion

FT-IR and FT-Raman spectra of 2-(benzylsulfanyl)-3,5-dinitrobenzoic acid were recorded and analyzed. SERS spectra were recorded in silver colloid, silver electrode and silver substrate. The vibrational wavenumbers were computed using HF and DFT basis sets. And potential energy distribution of the normal modes of vibrations was done using GAR2PED program. The geometrical parameters of the title compound are in agreement with the reported similar derivatives. The presence of phenyl ring modes in the SERS spectra suggests a tilted orientation with respect to the metal surface in all cases. In silver electrode and substrate phenyl ring PhII modes are additionally seen in the SERS spectra, which are absent in the SERS spectrum in silver colloid. It shows an orientation change in the electrode and substrate. In all the three SERS spectra the NO_2 moiety shows an enhancement, which indicates the interaction with the metal surface. The first hyperpolarizability is high and the title compound is an attractive object for future studies of nonlinear optics.

Acknowledgment

C. Yohannan Panicker would like to thank DST, India for a research grant.

References

[1] M. Moskovits, Rev. Mod. Phys. 57 (1985) 783–826.
[2] K. Kneipp, Y. Wang, H. Kneipp, L.T. Perelman, I. Itzkan, R.R. Dasari, M.S. Feld, Phys. Rev. Lett. 78 (1997) 1667–1670.
[3] K.C. Schuster, I. Reese, E. Urlaub, J.R. Gapes, B. Lendl, Anal. Chem. 72 (2000) 5529–5534.
[4] M.F. Erben, C.O.D. Vedova, R.M. Romano, R. Boese, H. Oberhammer, H. Willner, O. Sala, Inorg. Chem. 41 (2002) 1064–1071.
[5] S.T. Vallejos, M.F. Erben, H. Willner, R. Boese, C.O.D. Vedova, J. Org. Chem. 72 (2007) 9074–9080.
[6] X. Yang, X. Fang, X. Yang, M. Zhao, Y. Han, Y. Shen, F. Wu, Tetrahedron 64 (2008) 2259–2269.
[7] A.M. Venkatesan, J.M. Davis, G.T. Grosu, J. Baker, A. Zask, J.I. Levin, J. Ellingboe, J.S. Skotnicki, J.F. DiJoseph, A. Sung, G. Jin, W. Xu, D.J. McCarthy, D. Barone, J. Med. Chem. 47 (2004) 6255–6269.
[8] H. Pingali, M. Jain, S. Shah, S. Basu, P. Makadia, A. Goswami, P. Zaware, P. Patil, A. Godha, S. Giri, A. Goel, M. Patel, H. Patel, P. Patel, Bioorg. Med. Chem. Lett. 18 (2008) 5586–5590.
[9] T.M.C. Tan, Y. Chen, K.H. Kong, J. Bai, Y. Li, S.G. Lim, T.H. Ang, Y. Lam, Antiviral Res. 71 (2006) 7–14.
[10] Z. Abedinzadeh, Can. J. Physiol. Pharmacol. 79 (2001) 166–170.
[11] G.I. Giles, C. Jacob, Biol. Chem. 383 (2002) 375–388.
[12] O. Miyata, Y. Ozawa, I. Ninomiya, T. Naito, Tetrahedron 56 (2000) 6199–6207.
[13] O. Miyata, A. Nishiguchi, I. Ninomiya, K. Aoe, K. Okamura, T. Naito, J. Org. Chem. 65 (2000) 6922–6931.
[14] K.S. Feldman, A.L. Romanelli, R.E. Ruckle, R.F. Miller, J. Am. Chem. Soc. 110 (1988) 3300–3302.
[15] K.S. Feldman, C.J. Burns, J. Org. Chem. 56 (1991) 4601–4602.
[16] R. Pedrosa, C. Andres, J.P. Duque-Soladana, A. Maestro, J. Nieto, Tetrahedron: Asymmetry 14 (2003) 2985–2990.
[17] H. Hirt, R. Haemggi, J. Reyes, M. Seeger-Weibel, F. Gallou, Org. Process. Res. Dev. 12 (2008) 111–115.
[18] M.T. Ashby, H. Aneetha, J. Am. Chem. Soc. 126 (2004) 10216–10217.

[19] C. Ji, J.D. Goddard, A. Houmam, J. Am. Chem. Soc. 126 (2004) 8076–8077.
[20] C. Ji, M. Ahmida, M. Chahma, A. Houmam, J. Am. Chem. Soc. 128 (2006) 15423–15431.
[21] B.K. Sarma, G. Mugesh, J. Am. Chem. Soc. 129 (2007) 8872–8881.
[22] C.W. Wu, J.J. Ho, J. Org. Chem. 71 (2006) 9595–9601.
[23] E.W. Della, S.D. Graney, J. Org. Chem. 69 (2004) 3824–3835.
[24] L.H.J. Lajumen, P. Kokkonen, A. Nissi, H. Ruotsalainen, Thermochim. Acta 72 (1984) 219–224.
[25] D. Valigura, M. Melnik, M. Koman, L. Martiska, M. Korabik, J. Mrozinski, T. Glowiak, Polyhedron 23 (2004) 2447–2456.
[26] D. Valigura, M. Melnik, M. Koman, L. Martiska, M. Korabik, J. Mrozinski, T. Glowiak, Inorg. Chem. Commun. 7 (2004) 548–552.
[27] G. Smith, U.D. Wermuth, J.M. White, Acta Crystallogr. E57 (2001) 1036–1038.
[28] G. Smith, D.E. Lynch, K.A. Byriel, C.H.L. Kennard, Aust. J. Chem. 48 (1995) 1133–1149.
[29] V.S.S. Kumar, S.S. Kuduva, G.R. Desiraju, J. Chem. Soc. Perkin Trans. 2 (6) (1999) 1069–1074.
[30] A.A. Jbarah, K. Banert, R. Holze, Vib. Spectrosc. 44 (2007) 142–153.
[31] Y.R. Shen, The Principles of Nonlinear Optics, Wiley, New York, 1984.
[32] P.V. Kolinsky, Opt. Eng. 31 (1992) 1676–1684.
[33] D.F. Eaton, Science 253 (1991) 281–287.
[34] C.R. Moylan, R.J. Twieg, V.Y. Lee, S.A. Swanson, K.M. Betterton, R.D. Miller, J. Am. Chem. Soc. 115 (1993) 12599–12600.
[35] S. Gilmour, R.A. Montigomery, S.R. Marder, L.T. Cheng, A.K.Y. Je, Y. Cai, J.W. Perry, L.R. Dalton, Chem. Mater. 6 (1994) 1603–1604.
[36] C. Ravikumar, I.H. Joe, V.S. Jayakumar, Chem. Phys. Lett. 460 (2008) 552–558.
[37] P.C. Lee, D.J. Meisel, J. Phys. Chem. 86 (1982) 3391–3395.
[38] A. Kudelski, J. Bukowska, J. Raman Spectrosc. 26 (1995) 955–958.
[39] A. Kudelski, J. Bukowska, Surf. Sci. 368 (1996) 396–400.
[40] www.yashnanotech.com.
[41] M. Frisch, G.W. Trucks, H.B. Schlegel, G.E. Scuseria, M.A. Robb, J.R. Cheeseman, J.A. Montgomery Jr., T. Vreven, K.N. Kudin, J.C. Burant, J.M. Millam, S.S. Iyengar, J. Tomasi, V. Barone, B. Mennucci, M. Cossi, G. Scalmani, N. Rega, G.A. Petersson, H. Nakatsuji, M. Hada, M. Ehara, K. Toyota, R. Fukuda, J. Hasegawa, M. Ishida, T. Nakajima, Y. Honda, O. Kitao, H. Nakai, M. Klene, X. Li, J.E. Knox, H.P. Hratchian, J.B. Cross, C. Adamo, J. Jaramillo, R. Gomperts, R.E. Stratmann, O. Yazyev, A.J. Austin, R. Cammi, C. Pomelli, J.W. Ochterski, P.Y. Ayala, K. Morokuma, G.A. Voth, P. Salvador, J.J. Dannenberg, V.G. Zakrzewski, S. Dapprich, A.D. Daniels, M.C. Strain, O. Farkas, D.K. Malick, A.D. Rabuck, K. Raghavachari, J.B. Foresman, J.V. Ortiz, Q. Cui, A.G. Baboul, S. Clifford, J. Cioslowski, B.B. Stefanov, G. Liu, A. Liashenko, P. Piskorz, I. Komaromi, R.L. Martin, D.J. Fox, T. Keith, M.A. Al-Laham, C.Y. Peng, A. Nanayakkara, M. Challacombe, P.M.W. Gill, B. Johnson, W. Chen, M.W. Wong, C. Gonzalez, J.A. Pople, Gaussian 03, Revision C.02, Gaussian, Inc., Wallingford, CT, 2004.
[42] J.B. Foresman, in: E. Frisch (Ed.), Exploring Chemistry with Electronic Structure Methods: A Guide to Using Gaussian, Pittsburg, PA, 1996.
[43] J.M.L. Martin, C. Van Alsenoy, GAR2PEDA Program to obtain a Potential Energy Distribution from a Gaussian Archive Record, University of Antwerp, Belgium, 2007.
[44] N.P.G. Roeges, A Guide to the Complete Interpretation of Infrared Spectra of Organic Structures, Wiley, New York, 1994.
[45] A. Perjessy, D. Rasala, P. Tomasik, R. Gawinecki, Collect. Czech. Chem. Commun. 50 (1985) 2443–2452.
[46] N. Sundaraganesan, S. Ayyappan, H. Umamaheswari, B.D. Joshua, Spectrochim. Acta 66A (2007) 17–27.
[47] N.B. Colthup, L.H. Daly, S.E. Wiberly, Introduction to Infrared and Raman Spectroscopy, second ed., Academic Press, New York, 1985.
[48] R.M. Silverstein, G.C. Bassler, T.C. Morril, Spectrometic Identification of Organic Compounds (Ed. 5), John Wiley & Sons Inc., Singapore, 1991.
[49] D. Philip, A. John, C.Y. Panicker, H.T. Varghese, Spectrochim. Acta Part A 57 (2001) 1561–1566.
[50] C.Y. Panicker, H.T. Varghese, A. John, D. Philip, K. Istvan, G. Keresztury, Spectrochim Acta Part A 58 (2002) 281–287.
[51] H.T. Varghese, C.Y. Panicker, D. Philip, J. Chowdhury, M. Ghosh, J. Raman Spectrosc. 38 (2007) 323–331.
[52] P.L. Anto, C.Y. Panicker, H.T. Varghese, D. Philip, O. Temiz-Arpaci, B. Tekiner-Gulbaz, I. Yildiz, Spectrochim. Acta 67A (2007) 744–749.
[53] K.R. Ambujakshan, V.S. Madhavan, H.T. Varghese, C.Y. Panicker, O. Temiz-Arpaci, B. Tekiner-Gulbaz, I. Yildiz, Spectrochim. Acta 69A (2008) 782–788.
[54] P. Sett, N. Paul, S. Chattopadhyay, P.K. Mallick, J. Raman Spectrosc. 30 (1999) 277–287.
[55] V. Volovsek, G. Baranovic, L. Colombo, J.R. Durig, J. Raman Spectrosc. 22 (1991) 35–41.
[56] M. Muniz-Miranda, E. Castellucci, N. Neto, G. Sbrana, Spectrochim. Acta 39A (1983) 107–113.
[57] G. Varsanyi, Assignments of Vibrational Spectra of Seven Hundred Benzene Derivatives, Wiley, New York, 1974.
[58] G. Socrates, Infrared and Raman Characteristic Group Frequencies, Wiley, Middlesex, UK, 2001.
[59] R.D. Chambers, M.A. Fox, G. Sandford, J. Timicic, A. Goeta, J. Fluorine Chem. 128 (2007) 29–33.
[60] N. Okabe, T. Nakamura, H. Pukuda, Acta Crystallogr. C49 (1993) 1678–1680.
[61] M. Bujak, J. Zaleski, V. Preszhdo, B. Uspienskij, Acta Crystallogr. 58C (2002) 76–77.
[62] K. Siam, V.J. Klimkowski, J.D. Ewbank, C.V. Alsenoy, L. Schafter, J. Mol. Struct. 110 (1984) 171–182.
[63] C. Van Alsenoy, S. Kulp, K. Siam, V.J. Klimkowski, J.D. Ewbank, L. Schafer, J. Mol. Struct. Theochem. 181 (1988) 169–178.
[64] S.W. Ng, P. Naumov, M.G.B. Drew, G. Wojciehowski, B. Braezinski, J. Mol. Struct. 595 (2001) 29–37.
[65] J.A. Kaduk, Acta Crystallogr. 56B (2000) 474–485.
[66] M. Tommasini, C. Castiglioni, M. Del Zoppo, G. Zerbi, J. Mol. Struct. 480 (1999) 179–188.
[67] D.A. Kleinman, Phys. Rev. 126 (1962) 1977–1979.
[68] V.B. Jothy, T. Vijayakumar, V.S. Jayakumar, K. Udayalekshmi, K. Ramamoorthy, I.H. Joe, J. Raman Spectrosc. 38 (2007) 1148–1158.
[69] V. Krishnakumar, S. Dheivamalar, R.J. Xavier, V. Balachandran, Spectrochim. Acta 65A (2006) 147–154.
[70] G. Levi, J. Patigny, J.A. Massault, J. Aubard, in: 13th International Conference on Raman Spectroscopy, Wurzburg, 1992, p. 652.
[71] J.A. Creighton, Surf. Sci. 124 (1983) 209–219.
[72] J.S. Suh, M. Moskovits, J. Am. Chem. Soc. 108 (1986) 4711–4718.
[73] P. Gao, M.J. Weaver, J. Phys. Chem. 93 (1989) 6205–6211.
[74] M. Muniz-Miranda, Vib. Spectrosc. 29 (2002) 229–233.
[75] E.A. Carrasco, F.M. Campos-Vallette, P. Leyton, G. Diaz, R.E. Clavijo, J.V. Garcia-Ramos, N. Inostroza, C. Domingo, S. Sanchez-Cortes, R. Koch, J. Phys. Chem. 107 (2003) 9611–9619.
[76] P. Gao, M.J. Weaver, J. Phys. Chem. 89 (1985) 5040–5046.
[77] W. Ma, Y. Fang, J. Nanoparticle Res. 8 (2006) 761–767.
[78] J.A. Creighton, Spectroscopy of Surfaces-Advances in Spectroscopy, vol. 16, Wiley, New York, 1988. p. 37 (Chapter 2).
[79] X. Gao, J.P. Davies, M.J. Weaver, J. Phys. Chem. 94 (1990) 6858–6864.
[80] M. Moskovits, J.S. Suh, J. Phys. Chem. 88 (1984) 5526–5530.
[81] M. Moskovits, J.S. Suh, J. Phys. Chem. 92 (1988) 6327–6329.
[82] K. Eckhard, J.K. Bert, J.M. Robert, J. Phys. Chem. 100 (1996) 5078–5089.
[83] C. Frederico, G.J. Raul, C.N. Francisco, C. Paola, T. Marcia, J. Solid State Electrochim. 7 (2003) 576–581.
[84] K.A. Bunding, J.R. Lombardi, R.L. Birke, Chem. Phys. 49 (1980) 53–58.
[85] S. Kai, W. Chaozhi, X. Guangzhi, Spectrochim. Acta 45A (1989) 1029–1032.
[86] S.H. Han, I. Lee, K. Kim, Langmuir 28 (2002) 182–187.
[87] X.Y. Li, Q.Y. Huang, V.I. Petrov, Y.T. Xiu, Q. Luo, X. Yu, Y.J. Yan, J. Raman Spectrosc. 36 (2005) 555–573.
[88] N. Neto, M. Nocentini, M. Muniz-Miranda, G. Sbrana, J. Mol. Struct. 218 (1990) 423–428.
[89] P.J.G. Goulet, R.F. Aroca, Can. J. Chem. 82 (2004) 987–997.
[90] D. Sajan, I.H. Joe, V.S. Jayakumar, J. Zaleski, J. Chem. Sci. 120 (2008) 1–6.
[91] S. Sanchez-Cortes, J.V. Garcia-Ramos, J. Colloid Interface Sci. 231 (2000) 98–106.
[92] S. Sanchez-Cortes, O. Francioso, C. Ciavatta, J.V. Garcia-Ramos, C. Gessa, J. Colloid Interface Sci. 198 (1998) 308–318.
[93] K. Kneipp, R.R. Dasari, Y. Wang, Appl. Spectrosc. 48 (1994) 951–957.
[94] B. Giese, D. McNaughton, J. Phys. Chem. B106 (2002) 1461–1470.
[95] S.W. Joo, S.W. Han, H.S. Han, K. Kim, J. Raman Spectrosc. 31 (2000) 145–150.
[96] D.H. Son, S.J. Ahn, Y.J. Lee, K. Kim, J. Phys. Chem. 98 (1994) 8488–8493.
[97] Y.C. Liu, Langmuir 18 (2002) 174–181.
[98] Y.J. Kwon, D.H. Son, S.J. Ahn, M.S. Kim, K. Kim, J. Phys. Chem. 98 (1994) 8481–8487.
[99] Y. Wang, H. Chen, S. Dong, E. Wang, J. Raman Spectrosc. 39 (2008) 389–394.
[100] E. Podstawka, A. Kudelski, P. Kafarski, L.M. Proniewicz, Surf. Sci. 601 (2007) 4971–4983.